



NAVAL POSTGRADUATE SCHOOL

MONTEREY, CALIFORNIA

THESIS

**STUDY OF INTEGRATED USV/UUV OBSERVATION
SYSTEM PERFORMANCE IN MONTEREY BAY**

by

Christopher M. Bade

September 2017

Thesis Advisor:
Second Reader:

John Joseph
Tetyana Margolina

Approved for public release. Distribution is unlimited.

THIS PAGE INTENTIONALLY LEFT BLANK

REPORT DOCUMENTATION PAGE			Form Approved OMB No. 0704-0188
<p>Public reporting burden for this collection of information is estimated to average 1 hour per response, including the time for reviewing instruction, searching existing data sources, gathering and maintaining the data needed, and completing and reviewing the collection of information. Send comments regarding this burden estimate or any other aspect of this collection of information, including suggestions for reducing this burden, to Washington headquarters Services, Directorate for Information Operations and Reports, 1215 Jefferson Davis Highway, Suite 1204, Arlington, VA 22202-4302, and to the Office of Management and Budget, Paperwork Reduction Project (0704-0188) Washington, DC 20503.</p>			
1. AGENCY USE ONLY (Leave blank)	2. REPORT DATE	3. REPORT TYPE AND DATES COVERED	
	September 2017	Master's thesis	
4. TITLE AND SUBTITLE STUDY OF INTEGRATED USV/UUV OBSERVATION SYSTEM PERFORMANCE IN MONTEREY BAY		5. FUNDING NUMBERS	
6. AUTHOR(S) Christopher M. Bade			
7. PERFORMING ORGANIZATION NAME(S) AND ADDRESS(ES) Naval Postgraduate School Monterey, CA 93943-5000		8. PERFORMING ORGANIZATION REPORT NUMBER	
9. SPONSORING /MONITORING AGENCY NAME(S) AND ADDRESS(ES) N/A		10. SPONSORING / MONITORING AGENCY REPORT NUMBER	
<p>11. SUPPLEMENTARY NOTES The views expressed in this thesis are those of the author and do not reflect the official policy or position of the Department of Defense or the U.S. Government. IRB number _____ N/A.</p>			
12a. DISTRIBUTION / AVAILABILITY STATEMENT Approved for public release. Distribution is unlimited.		12b. DISTRIBUTION CODE	
<p>13. ABSTRACT (maximum 200 words)</p> <p>This study tests the feasibility of using a system of integrated unmanned underwater vehicles (UUVs) and unmanned surface vehicles (USVs) in support of long-endurance oceanographic characterization and acoustic source detection and tracking. Such a system would have the potential to enable long-residence acoustic and oceanographic sampling while providing the opportunity for broad area acoustic coverage and source track resolution with a small number of UUVs using a technique of sequential localization developed by Chan and Towers in 1992. The performance of an underwater glider-based detection system was tested in Monterey Bay using a programmable mobile acoustic source. Multiple subsurface acoustic hydrophones configured similarly to a proposed array of gliders were used to test tracking of the medium frequency source and other performance characteristics.</p> <p>Analysis of recorded Doppler shifts demonstrated closest point of approach (CPA) values consistent with source tracks in both course and speed. A notional sensor layout for the proposed integrated system was demonstrated to show optimal track reconstruction. Factors degrading the ability of this method to make accurate CPA estimates were also explored. The results of this study demonstrate the feasibility of using a system of UUVs/USVs for persistent acoustic sensing and tracking leveraging the characteristics of long-residence time and broad area coverage.</p>			
14. SUBJECT TERMS acoustics, unmanned systems, Doppler, maritime surveillance, UUV, oceanographic sampling, passive acoustics, acoustic localization			15. NUMBER OF PAGES 45
			16. PRICE CODE
17. SECURITY CLASSIFICATION OF REPORT Unclassified	18. SECURITY CLASSIFICATION OF THIS PAGE Unclassified	19. SECURITY CLASSIFICATION OF ABSTRACT Unclassified	20. LIMITATION OF ABSTRACT UU

THIS PAGE INTENTIONALLY LEFT BLANK

Approved for public release. Distribution is unlimited.

**STUDY OF INTEGRATED USV/UUV OBSERVATION SYSTEM
PERFORMANCE IN MONTEREY BAY**

Christopher M. Bade
Lieutenant Commander, United States Navy
B.S., Oklahoma State University, 1999
Ph.D., Ohio University, 2006

Submitted in partial fulfillment of the
requirements for the degree of

**MASTER OF SCIENCE IN METEOROLOGY AND
PHYSICAL OCEANOGRAPHY**

from the

**NAVAL POSTGRADUATE SCHOOL
September 2017**

Approved by: John Joseph
 Thesis Advisor

Tetyana Margolina
Second Reader

Peter Chu
Chair, Department of Oceanography

THIS PAGE INTENTIONALLY LEFT BLANK

ABSTRACT

This study tests the feasibility of using a system of integrated unmanned underwater vehicles (UUVs) and unmanned surface vehicles (USVs) in support of long-endurance oceanographic characterization and acoustic source detection and tracking. Such a system would have the potential to enable long-residence acoustic and oceanographic sampling while providing the opportunity for broad area acoustic coverage and source track resolution with a small number of UUVs using a technique of sequential localization developed by Chan and Towers in 1992. The performance of an underwater glider-based detection system was tested in Monterey Bay using a programmable mobile acoustic source. Multiple subsurface acoustic hydrophones configured similarly to a proposed array of gliders were used to test tracking of the medium frequency source and other performance characteristics.

Analysis of recorded Doppler shifts demonstrated closest point of approach (CPA) values consistent with source tracks in both course and speed. A notional sensor layout for the proposed integrated system was demonstrated to show optimal track reconstruction. Factors degrading the ability of this method to make accurate CPA estimates were also explored. The results of this study demonstrate the feasibility of using a system of UUVs/USVs for persistent acoustic sensing and tracking leveraging the characteristics of long-residence time and broad area coverage.

THIS PAGE INTENTIONALLY LEFT BLANK

TABLE OF CONTENTS

I.	INTRODUCTION.....	1
II.	BACKGROUND.....	3
	A. MOTIVATION FOR UNMANNED SYSTEMS	3
	B. STUDY PROPOSAL	3
	C. DESIRED OPERATION	4
III.	DISCUSSION.....	5
IV.	EXPERIMENTAL SETUP	7
	A. MONTEREY BAY EXPERIMENT	7
	1. Source	7
	2. Receivers.....	7
	B. NOTIONAL SENSOR DEPLOYMENT.....	10
V.	RESULTS	11
	A. NOTIONAL EXPERIMENT	11
	B. DATA ANALYSIS	12
	1. Data Selection.....	12
	2. Selected Cases	14
	C. RECONSTRUCTION OF EMATT TRACK.....	23
	D. SPEED DETERMINATION	24
VI.	CONCLUSIONS.....	25
	LIST OF REFERENCES.....	27
	INITIAL DISTRIBUTION LIST	29

THIS PAGE INTENTIONALLY LEFT BLANK

LIST OF FIGURES

Figure 1.	Theoretical Frequency Response for a 3 kHz Source Moving at 5 kts and Stationary Receiver at Various CPAs	6
Figure 2.	Acousonde 3A Broadband Receiver. Adapted from Acoustimetrics (2013).....	8
Figure 3.	MARS Observatory Science Node. Source: MBARI (2017a).	9
Figure 4.	MARS Hydrophone. Adapted from MBARI (2017b).....	9
Figure 5.	Notional Sensor Layout.....	10
Figure 6.	Sequential Localization Source Track Reconstruction Using Notional Sensor Layout	12
Figure 7.	Spectrogram Demonstrating Erratic Behavior of EMATT	13
Figure 8.	Spectrogram of Multiple Passes Recorded on MARS Receiver	15
Figure 9.	Spectrogram with Broadband Noise during CPA and Low SNR....	16
Figure 10.	Frequency-Time Plot with Broadband Noise during CPA and Low SNR	17
Figure 11.	Frequency-Time Plot with Broadband Noise during CPA and Low SNR and More Smoothing	17
Figure 12.	Spectrogram Resulting in a Successful Curve Fit	18
Figure 13.	Frequency-Time Fit with Lower Value of Running Average Smoothing	19
Figure 14.	Frequency-Time Fit with Larger Value of Running Average Smoothing	19
Figure 15.	Spectrogram with Fadeout	21
Figure 16.	Time-Frequency Plot with Fadeout.....	21
Figure 17.	Spectrogram with More Signal Uncertainty	22
Figure 18.	Frequency-Time Plot With Greater Signal Uncertainty	22

Figure 19. Programmed EMATT Track and Sensor Layout with CPA
Range Circles 24

LIST OF ACRONYMS AND ABBREVIATIONS

ASW	antisubmarine warfare
CPA	closest point of approach
EMATT	expendable mobile ASW training target
MARS	Monterey Accelerated Research System
MBARI	Monterey Bay Aquarium Research Institute
PSD	power spectral density
SNR	signal-to-noise ratio
USV	unmanned surface vehicle
USW	undersea warfare
UUV	unmanned underwater vehicle

THIS PAGE INTENTIONALLY LEFT BLANK

ACKNOWLEDGMENTS

This work would not have been possible without the enormous support of my wife, Cheryl. I would like to thank the faculty and staff of Naval Postgraduate School, particularly John Joseph and Tetyana Margolina. My program officer, Commander Paula Travis, provided needed support as well. The Naval Postgraduate School faculty and staff are incredibly professional and knowledgeable.

The Monterey Bay Aquarium Research Institute provided acoustic data captured by the Monterey Accelerated Research System as well as other technical support for this work.

THIS PAGE INTENTIONALLY LEFT BLANK

I. INTRODUCTION

This study builds on work by Nott (2015) testing glider systems in Monterey Bay to develop integrated unmanned surface vehicle (USV)/unmanned underwater vehicle (UUV) systems. Many of the goals remain the same and within reach. Advanced technologies in glider payload research have been demonstrated by Maguer et al. (2013).

Oceanographic and acoustic sampling remain critical components of the United States Navy undersea warfare (USW) mission. UUVs have the advantage of long endurance and can persist quasi-stationary at depth in low-current environments.

This thesis evaluates the performance of deep sensors in determining behavior of a moving source utilizing a technique of sequential localization from Doppler shifted frequency measurements (Chan and Towers 1992). Sensitivity of various parameters to source and receiver configuration is also explored.

While the feasibility of operating an integrated USV/UUV observation system is demonstrated here, additional integration of acoustic communication, onboard signal processing, and submerged command and control requires further study.

THIS PAGE INTENTIONALLY LEFT BLANK

II. BACKGROUND

A. MOTIVATION FOR UNMANNED SYSTEMS

The use of UUVs for long-duration, wide-area oceanographic surveillance and environmental characterization is well established. Recent work has demonstrated expanding the mission set for UUV gliders by adding payloads capable of passive acoustic monitoring, sea bottom characterization, and acoustic modem communication (Send et al. 2013, Maguer et al. 2013, Baumgartner et al. 2014).

Combining some of these new capabilities with existing ocean glider capability makes an integrated system of UUVs providing wide-area, long-duration oceanographic and environmental sensing capability extremely attractive for capability of performing the United States Navy USW mission.

B. STUDY PROPOSAL

In support of recent initiatives from the Deputy Chief of Naval Operations for Information Warfare (N2/N6) to study environmental sensing through the integration of USVs and UUVs, researchers at Naval Postgraduate School submitted a research proposal to use those vehicles in an integrated, long-residence network for oceanographic and acoustic characterization and undersea surveillance (Joseph and Horner 2014). This thesis follows the work of Nott (2015) in support of studying the use of UUV/USVs for these purposes. While Nott studied glider-based passive acoustic detection, this thesis expands on that work by exploring a method of determining source behavior through frequency Doppler shift measurements with detectors placed as a widely distributed UUV array would be for a fully developed system.

C. DESIRED OPERATION

An ideal system of networked USV/UUVs would be semi-autonomous. A distributed, reliable network of UUVs could be remotely operated by ship-based or shore-based command and control of the USV. UUVs need to be able to drift at depth where signal-to-noise ratio (SNR) is favorable for acoustic collection and characterization for long periods vice frequently surfacing to transmit data and receive commands. UUVs would retain their present oceanographic sampling capability while performing this additional function. USVs or other similar control nodes must be able to synthesize information and develop an overall operational picture. This thesis explores one method of combining acoustic information from multiple sensors without onerous requirements of precise time synchronization. Methods for maximizing the coverage area of a fixed number of units or reducing the number of units for a given coverage area should be developed.

III. DISCUSSION

A receiver will experience a Doppler shift in frequency received relative to a source transmission frequency when the source and receiver are moving relative to each other. Equation 1 states the received frequency relationship to the source frequency where c is the speed of sound in water, u is the source speed, and v is the receiver speed:

$$f_r = f_0 \frac{c + u \cos \theta_s}{c + v \cos \theta_r}. \quad (1)$$

If one assumes a stationary receiver and a mobile source travelling linearly at constant depth, Equation 1 can be rewritten in terms of the closest point of approach (CPA), d , between the source and the receiver and the distance along the source's track, x , from the point of closest approach. This relationship is given in Equation 2:

$$f_r = f_0 \frac{c + u \frac{x}{\sqrt{x^2 + d^2}}}{c}. \quad (2)$$

Rewriting x in terms of time ($t=0$ when $x=0$) for constant u yields Equation 3:

$$f_r = f_0 \frac{c + \frac{u^2 t}{\sqrt{u^2 t^2 + d^2}}}{c}. \quad (3)$$

Some examples of theoretical time-frequency plots are shown in Figure 1 for various CPA distances. As CPA distances increase, the inflection point approximates linear behavior for longer periods. As CPA distances decrease, the change in concavity of the function is more dramatic and localized. This function can be expanded as a linear approximation near the point of closest approach if the source velocity is known.

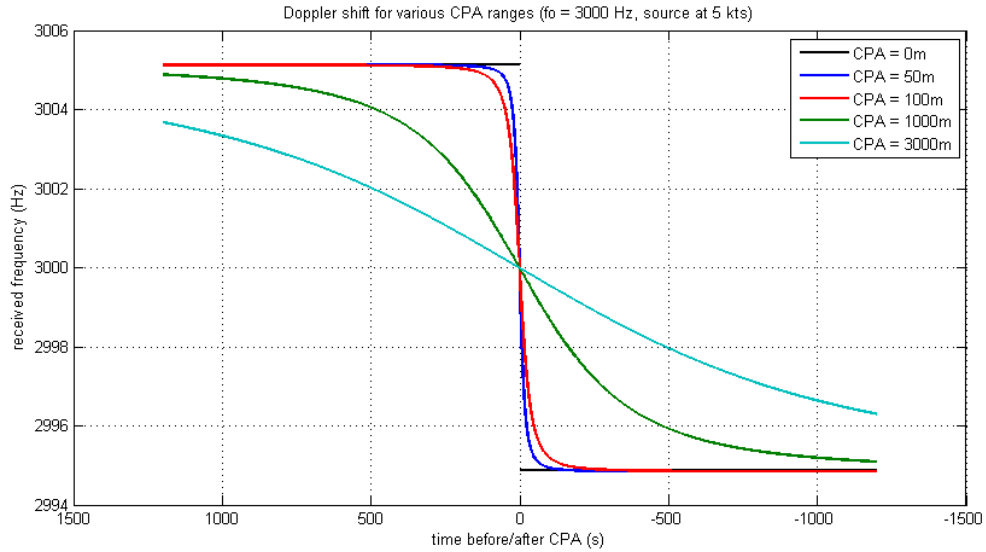


Figure 1. Theoretical Frequency Response for a 3 kHz Source Moving at 5 kts and Stationary Receiver at Various CPAs

Chan and Towers (1992) described a technique for using three or more omni-directional sensors to localize a linearly traveling source using determination of closest point of approach and speed of a constant frequency source for three or more sensors and then reconstructing the source track based on that information. This technique is directly applicable to integrated UUVs carrying acoustic sensors that would be quasi-stationary receivers when in drift mode at depth in low current environments. One key advantage to this technique is that, unlike traditional arrays of hydrophones, precise time synchronization is not required for spatial beamforming.

IV. EXPERIMENTAL SETUP

A. MONTEREY BAY EXPERIMENT

Receivers were arranged in a configuration similar to how integrated UUV sensors would be deployed, one on a UUV, and other spatially separated submerged receivers. A programmable antisubmarine warfare (ASW) training target was used as the mobile acoustic source.

1. Source

The sources used for this study were MK39 expendable mobile ASW training target (EMATT) drones. They are programmable in acoustic source characteristics and movement profile and can be operated for as long as 8 hours covering optimal range, making them convenient for testing acoustic detection techniques. For this study, the EMATT was programmed to travel back and forth on a single transect at different depths during each pass. It transmitted a 950 Hz narrowband signal throughout the test and additionally transmitted individual narrowband frequencies each pass ranging from 2700 Hz to 3000 Hz.

2. Receivers

a. *Acousonde*

A broadband omnidirectional acoustic recorder made by Acoustimetrics (2013) was mounted on a Spray glider for this study. The model used was the Acousonde 3A. Three additional acousondes were deployed tethered to surface buoys during the first day of data collection and recovered when testing was complete. While the receiver on the Spray glider was in position for the study, mechanical problems on our research vessel prevented deploying these additional sensors the second day of data collection. We were still able to deploy the EMATT for data collection by the available sensors before returning to shore however. Figure 2 shows the dimensions and components.

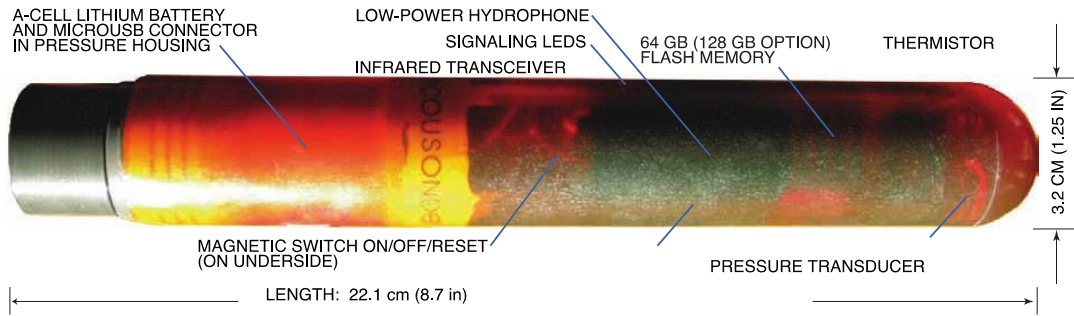
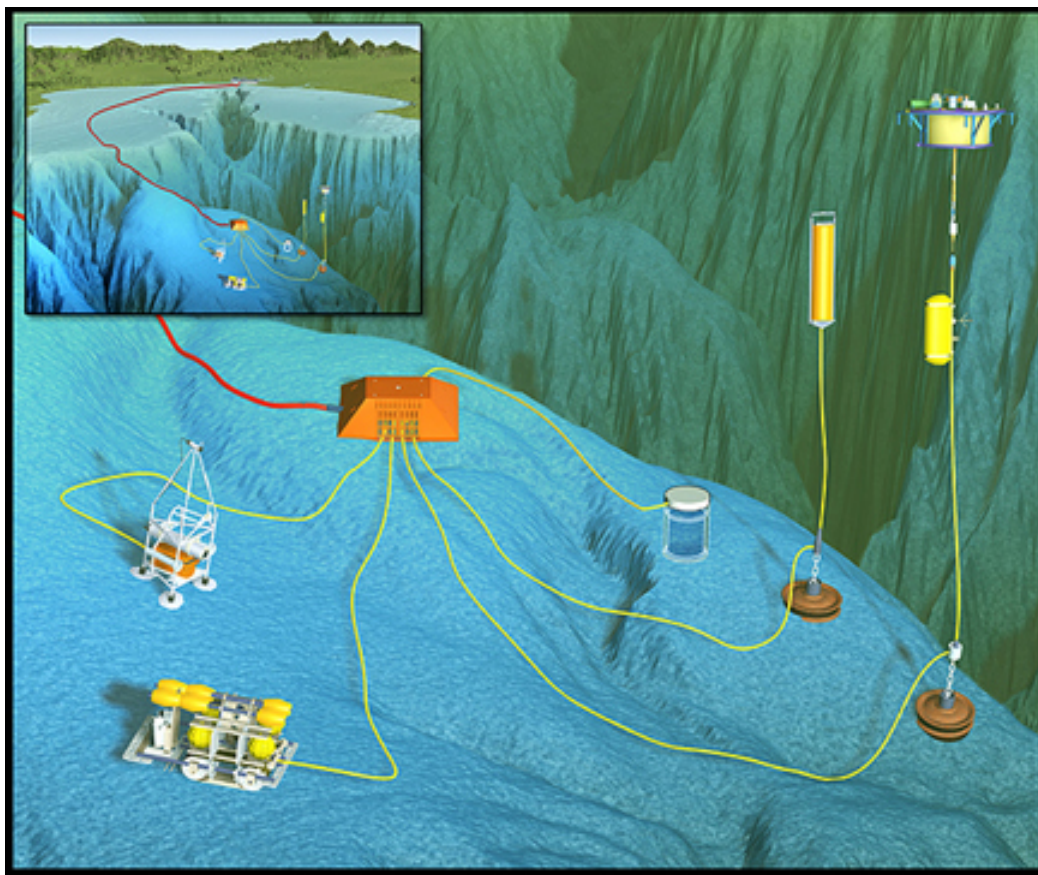


Figure 2. Acousonde 3A Broadband Receiver. Adapted from Acoustimetrics (2013).

b. MARS Hydrophone

The Monterey Bay Aquarium Research Institute (MBARI) has deployed a cabled observatory called the Monterey Accelerated Research System (MARS) cabled observatory in Monterey Bay shown in Figure 3. Of note, MARS has a digital broadband hydrophone deployed at 900 m depth shown in Figure 4 (MBARI 2017b). The hydrophone was deployed to record a broad range of marine sounds produced by natural and manmade processes. The instrument records at a sampling rate of over 250 kHz and can continuously record and collect data due to the cabled nature of the observatory (MBARI 2017b). MBARI has made the acoustic data collected during this experiment available for this study. This provides not only a sensor of opportunity, but serves as an approximation of a stationary hydrophone at depths similar to proposed glider operation.



"The MARS observatory 'science node' (shown in orange) has eight ports, each of which can supply data and power connections for a variety of scientific instruments. Scientists have constant access to their experiments through the seafloor cable."

Figure 3. MARS Observatory Science Node. Source: MBARI (2017a).

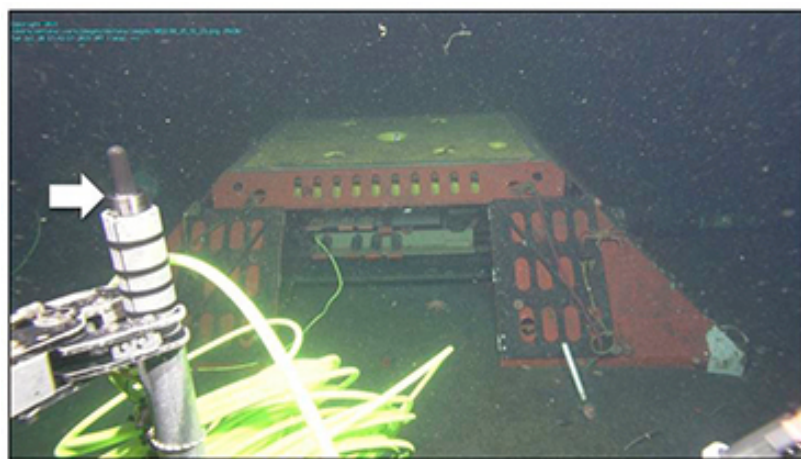


Figure 4. MARS Hydrophone. Adapted from MBARI (2017b).

B. NOTIONAL SENSOR DEPLOYMENT

Because the use of a system of glider-mounted Acousondes is currently in testing and development, a notational sensor deployment is proposed, using more submerged sensors than were available for this study. An ideal setup would have the source track passing sensors at different times with different CPA distances and that the receivers be arranged around an anticipated source track. Figure 5 shows a notional sensor layout for the experimental area. The black diamonds indicate possible sensor positions for monitoring the source during the north-south portion of the blue track. For simplicity, the sensors can be all placed at the same depth.

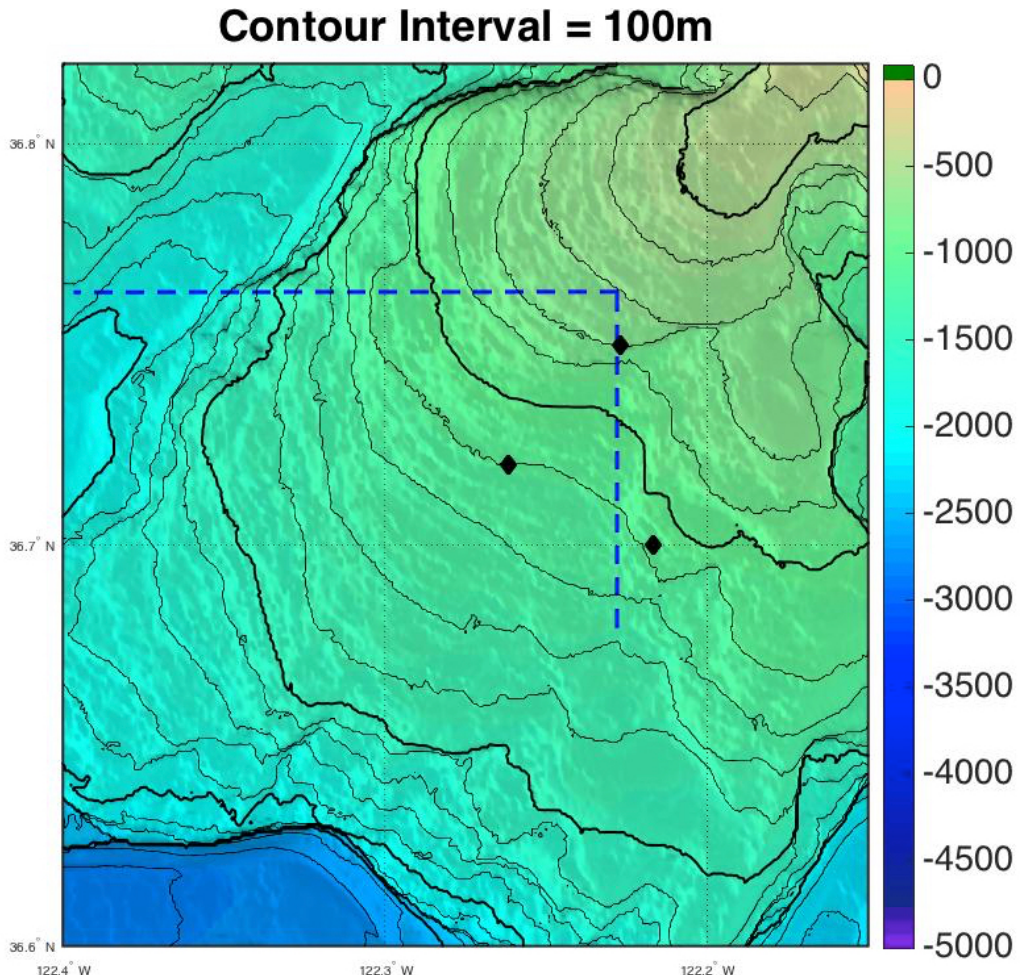


Figure 5. Notional Sensor Layout

V. RESULTS

A. NOTIONAL EXPERIMENT

The demonstration of reconstruction of a moving source track using a notional sensor placement is shown in Figure 6. As described by Chan and Towers (1992), a sufficient number of sensors can determine a linearly travelling source track. Chan and Towers (1992) showed the minimum number of separate receivers to determine the source track is three. Placing acoustic sensors closer to the source track will allow for lower uncertainty in parameter estimation using non-linear regression, but to have an unambiguous result, the track must travel through the field of sensors. A wider field of sensors makes it more likely the source track will travel between them.

The red circles in Figure 6 indicate the set of possible locations of the source at the time of CPA for each sensor. These circles are constructed given “perfect data” of the theoretical frequency-time plots in Figure 1 for the 3000m, 1000m, and 100m distance of closest approach cases. By knowing the individual CPAs for each sensor, the source track would then be able to be reconstructed through sequential localization, not requiring that all sensors be in contact with the source at the same time or requiring as many sensors as you would for a single simultaneous measurement (Chan and Towers, 1992). For a linearly travelling constant-depth source, the three red circles determine the path of the source.

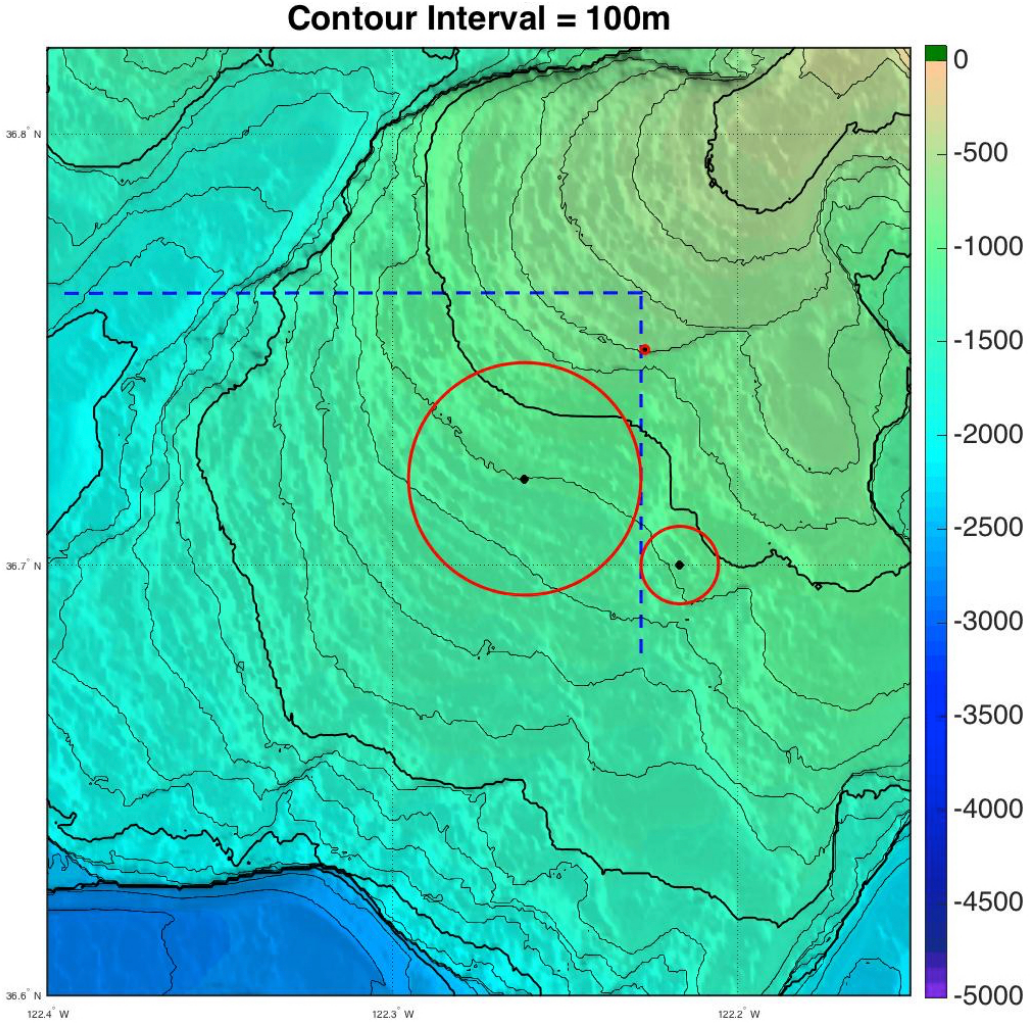


Figure 6. Sequential Localization Source Track Reconstruction Using Notional Sensor Layout

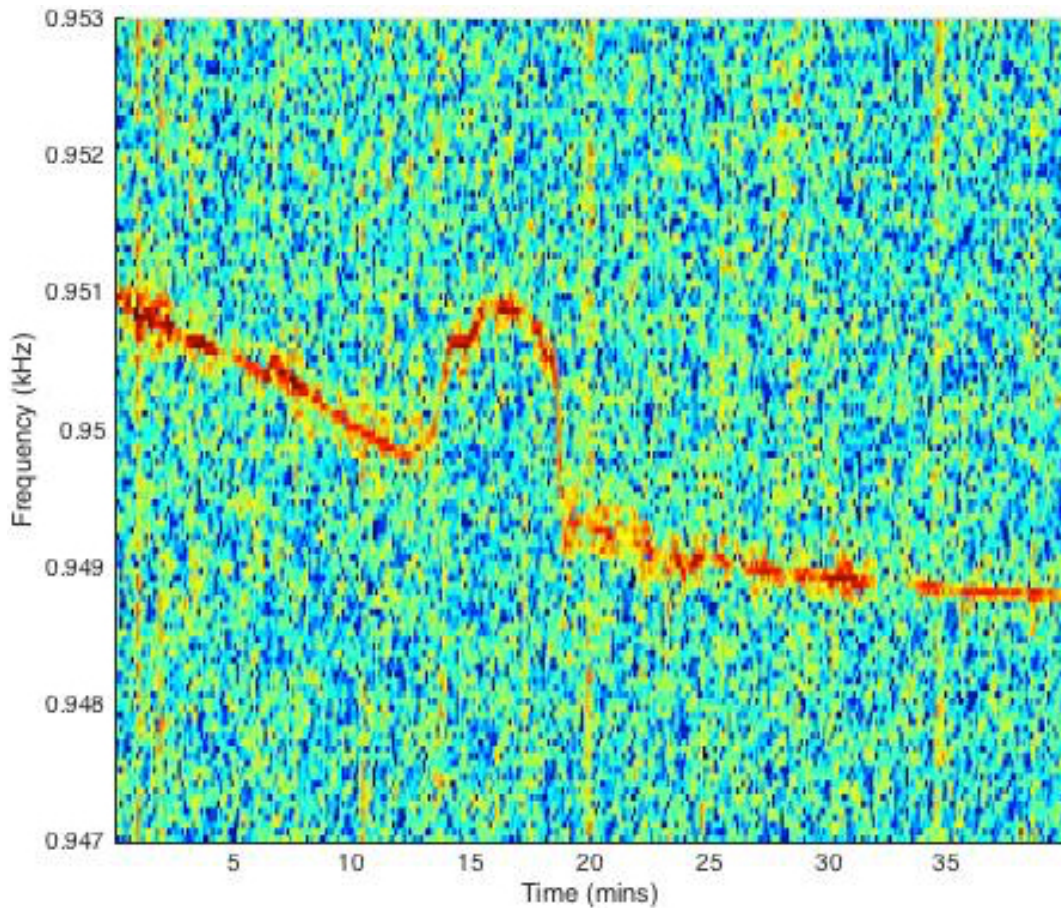
B. DATA ANALYSIS

1. Data Selection

As noted in Experimental Setup, the second day of data collection did not include the intended buoy-mounted receivers. Unfortunately during the first day of collection, subsequent acoustic analysis revealed the EMATT did not behave as programmed. The data were consistent with the EMATT performing uncommanded turns vice travelling in a straight line at constant bearing. An example of this erratic behavior is shown in Figure 7. Additionally, the EMATT

stopped transmitting abruptly after a broadband spike in noise, indicating a likely catastrophic failure.

On the second day, the availability of the glider acousonde and MARS data resulted in enough acoustic sensor data being collected for demonstration of this feasibility study, however.



The frequency jump at 13 mins does not correspond to a constant-frequency source travelling in a straight-line direction as the curves in Figure 1. Possible causes are the source changing direction, speed, or transmitted frequency.

Figure 7. Spectrogram Demonstrating Erratic Behavior of EMATT

2. Selected Cases

Acoustic signals detected by the hydrophone sensors were converted to spectrograms through a fast Fourier transform (FFT) with about .1 Hz resolution calculating power spectral densities (PSD) on ten seconds of data with 90% overlap, yielding about 1 second time resolution. This high frequency and time resolution is necessary to determine the subtle frequency shifts due to the speed of the source. Doppler shifts of less than 1 percent of the source frequency are normal and expected. The sound pressure level units for the acousonde are dB re 1 μ Pa. The MARS hydrophone data are scaled by an arbitrary gain, but only signal-to-noise ratio is important for this study. Using a narrow frequency band around the source frequency, the frequency of maximum sound pressure level for each time was extracted to reveal a time-frequency relationship similar in form to the theoretical curves shown in Figure 1. Some smoothing using a running average was applied to the time-frequency plots and then non-linear regression was used to fit the frequency curve to Equation 3 and determine the speed of the source as well as the distance of closest approach. In all plots, the blue curve is the frequency-time data and the red curve is the resulting nonlinear regression fit to the data. The parameters of speed and distance of closest approach were estimated and 95% confidence intervals were generated. The central frequency parameter was used as an additional diagnostic to indicate when poor fits yielded suspect parameter estimates, i.e., a central frequency “miss” would indicate unreliable results. Figure 8 shows an example of a spectrogram with multiple source passes by the MARS receiver. Each pass was examined separately.

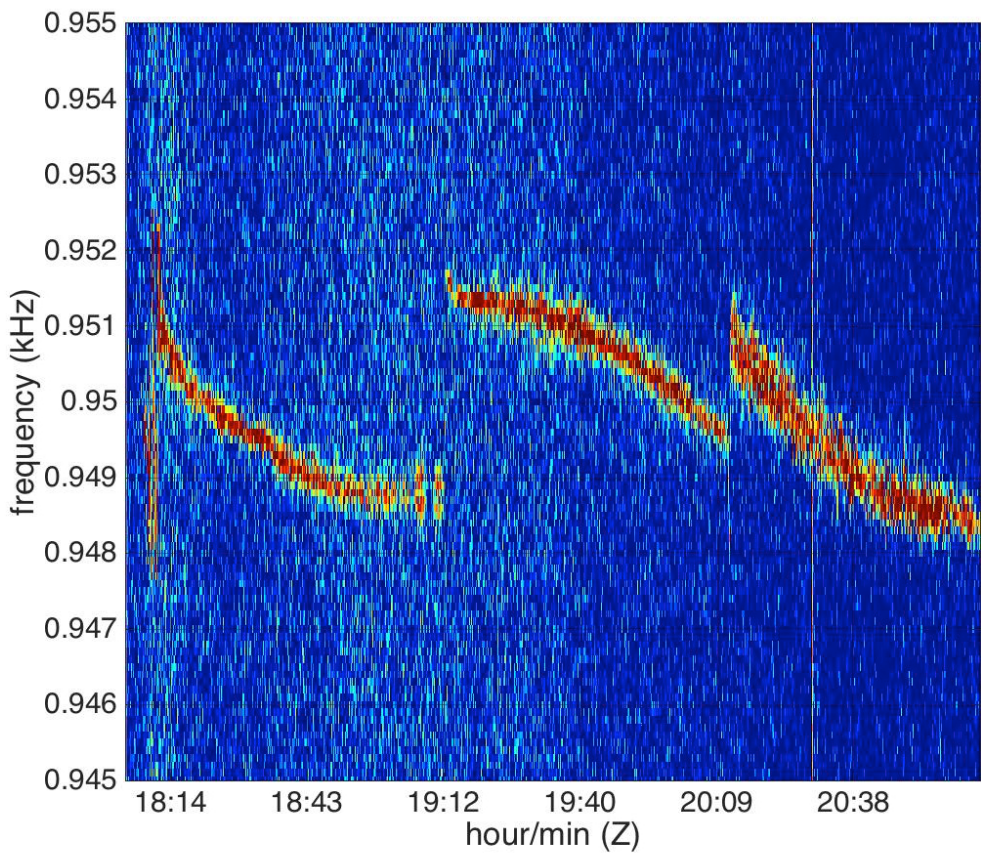
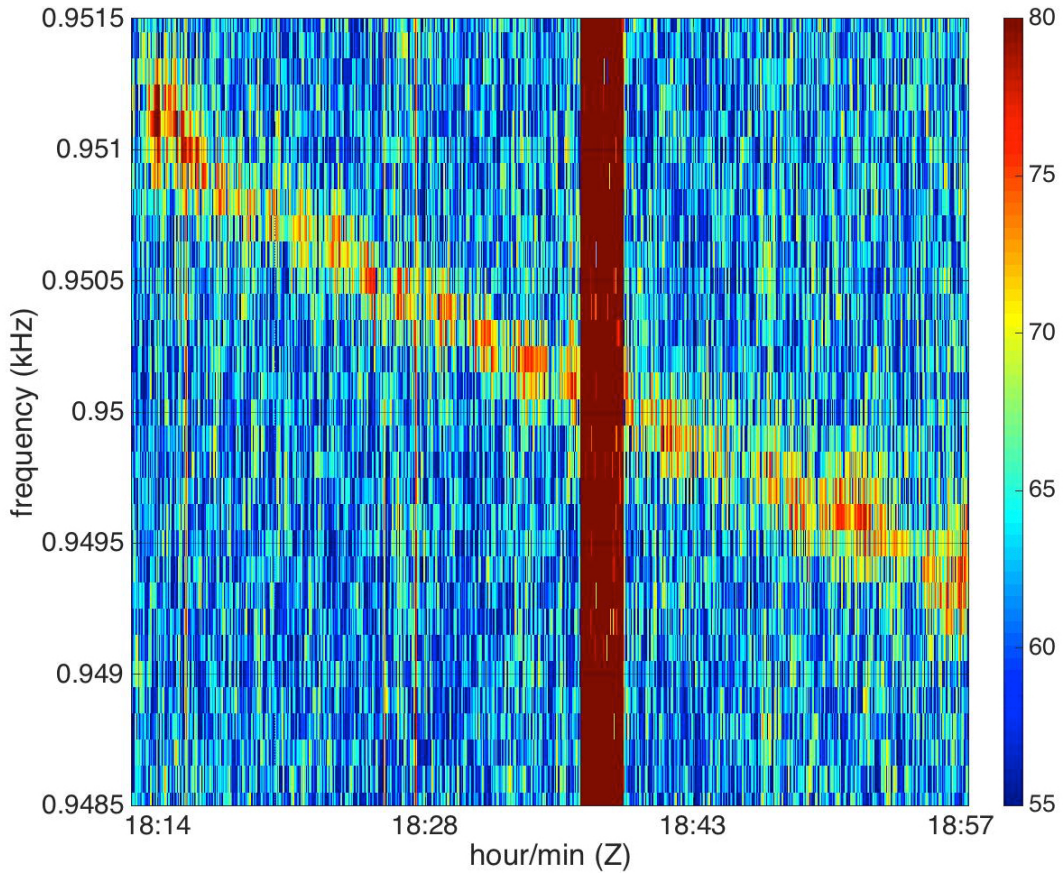


Figure 8. Spectrogram of Multiple Passes Recorded on MARS Receiver

Assumptions required to perform the regression technique were quasi-stationary receivers, a constant-depth linearly traveling source for each pass, and a known source frequency. The MARS receiver was certainly stationary during the experiment. Assuming the sensor mounted on the glider was stationary during drift mode is safe since the currents at depth in Monterey Bay are much lower than the speed of the source. The EMATT was programmed in frequency transmission and motion profile to conform to the experimental assumptions. Some example spectra and frequency-time fits are shown here to demonstrate advantages and limitations of this technique.

a. Low SNR, Broadband Noise at CPA

Figure 9 is a spectrogram for an EMATT pass of the acousonde located on the UUV. The signal to noise ratio is low and there is a broadband self-noise event on the glider during CPA. Figures 10 and 11 are corresponding time-frequency plots with different levels of moving average smoothing. Curve fits are shown on these plots and are poor due to the low SNR and lack of data at the crucial time of CPA. The parameter estimates that resulted had orders of magnitude of uncertainty for their respective values. A mismatch of the central frequency and the resulting zero time provides an indication of failure of the parameter estimation technique in this case.



The red vertical bar is a broadband noise spike right at the moment of crossing the central frequency (CPA).

Figure 9. Spectrogram with Broadband Noise during CPA and Low SNR

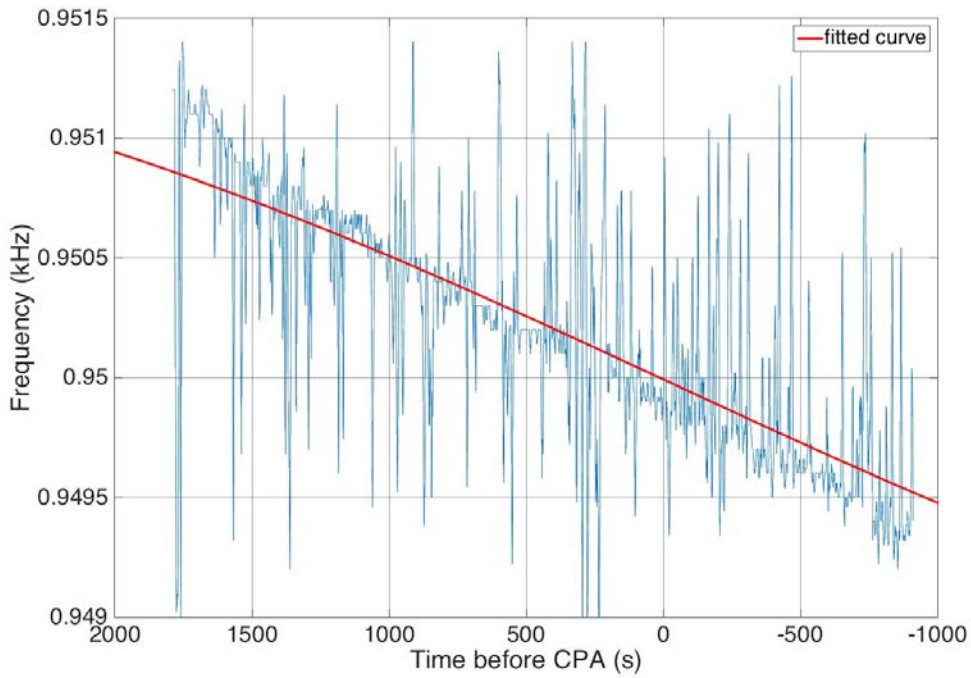
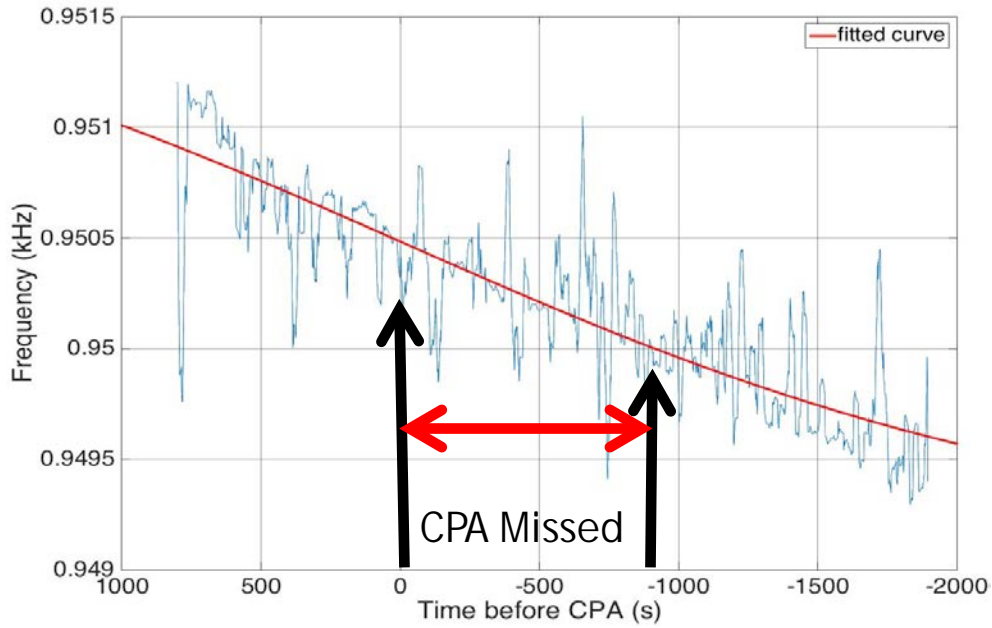


Figure 10. Frequency-Time Plot with Broadband Noise during CPA and Low SNR



The mismatch between $t=0$ and the central frequency (0.95 kHz) indicates a problem with the nonlinear regression result in this case

Figure 11. Frequency-Time Plot with Broadband Noise during CPA and Low SNR and More Smoothing

b. Successful Curve Fit

Figure 12 shows the spectrogram used to generate Figures 13 and 14. Again these Figures respectively correspond to less and more smoothing. The curve fit matches the data much better than the previous case and is used to estimate the distance of closest approach for this EMATT pass. This fit yielded an EMATT speed value of 2.67 m/s and a slant-range distance of 5303 m. The 95% confidence interval for speed was less than 1% of the value and ~2.5% for slant-range distance in this case.

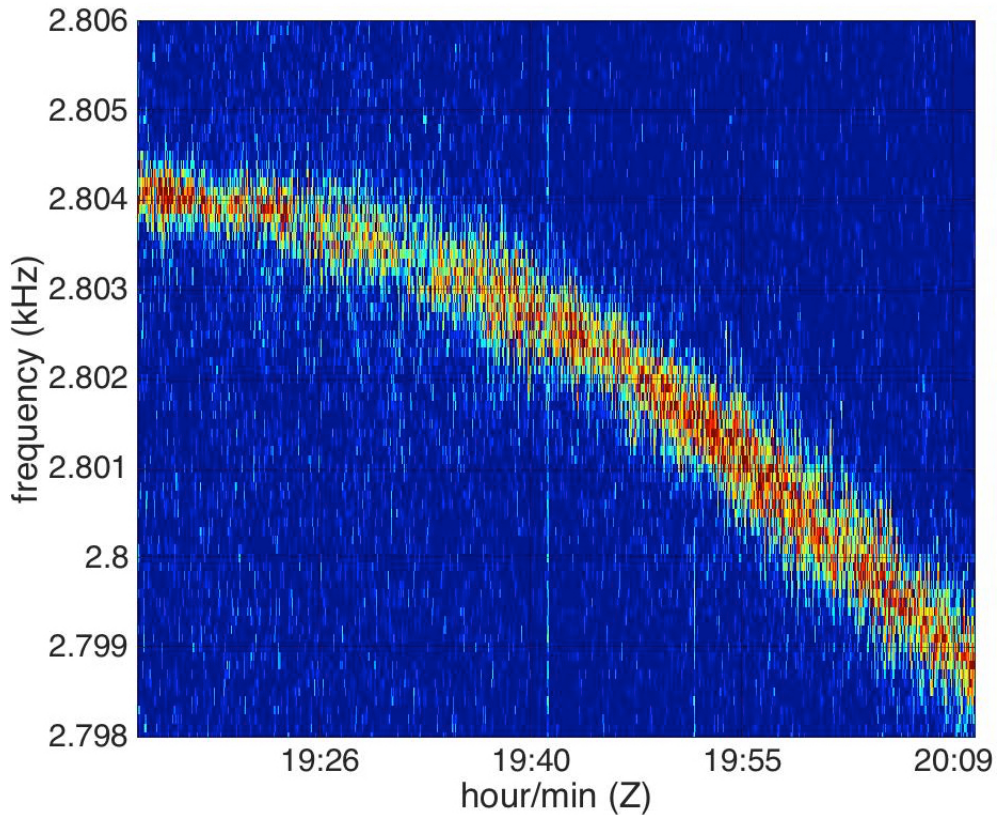


Figure 12. Spectrogram Resulting in a Successful Curve Fit

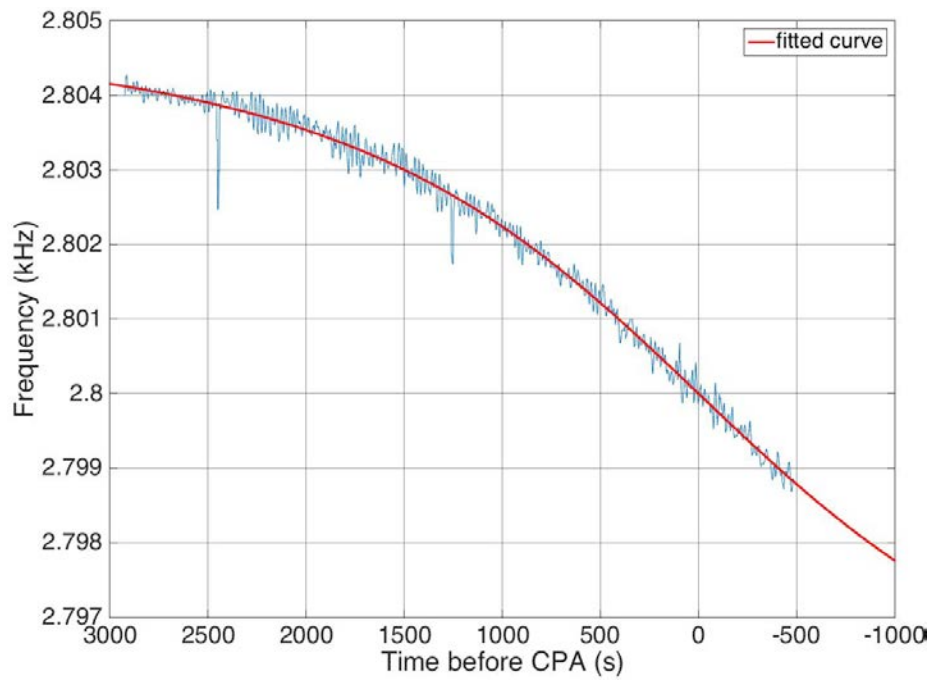


Figure 13. Frequency-Time Fit with Lower Value of Running Average Smoothing

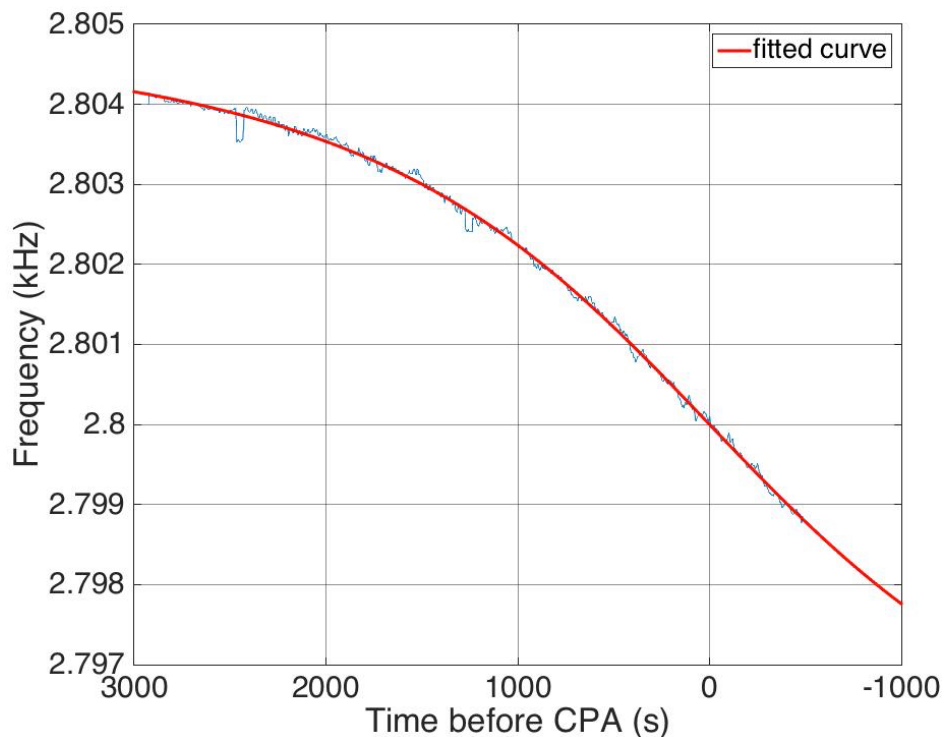


Figure 14. Frequency-Time Fit with Larger Value of Running Average Smoothing

c. Near Surface Fadeout

Figure 15 is a spectrogram showing the signal fading out during the pass, probably due to some transmission loss transient. Figure 16 plots the corresponding time-frequency dependence and curve fit. The fadeout introduces additional noise and prevents a successful curve fit. Confidence intervals covered multiple orders of magnitude and resulting speed values were unreasonably fast.

For the same pass, a lower frequency of 950 Hz was also transmitted by the source. As shown in Figures 17 and 18, the received signal at this frequency does not experience the same fadeout, but the signal is much broader than other passes. This pass was run at a shallower EMATT depth, so it is likely that interaction with surface reflection or greater ambient noise reduced the quality of the received signal.

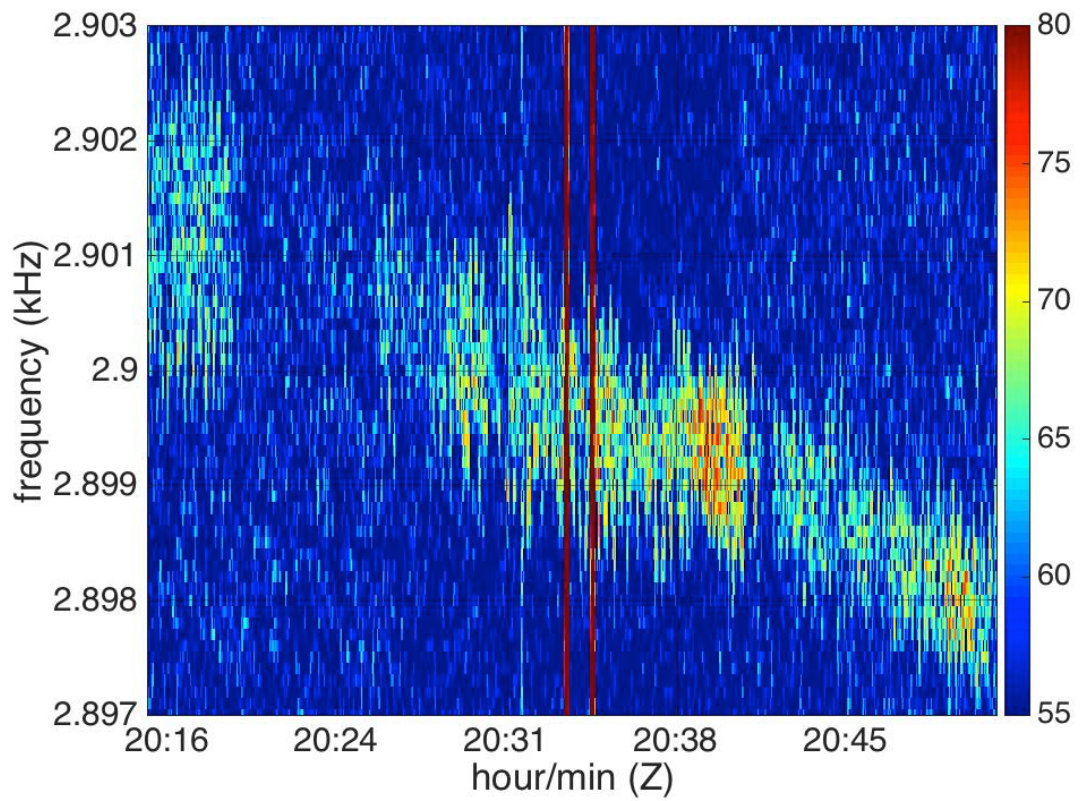


Figure 15. Spectrogram with Fadeout

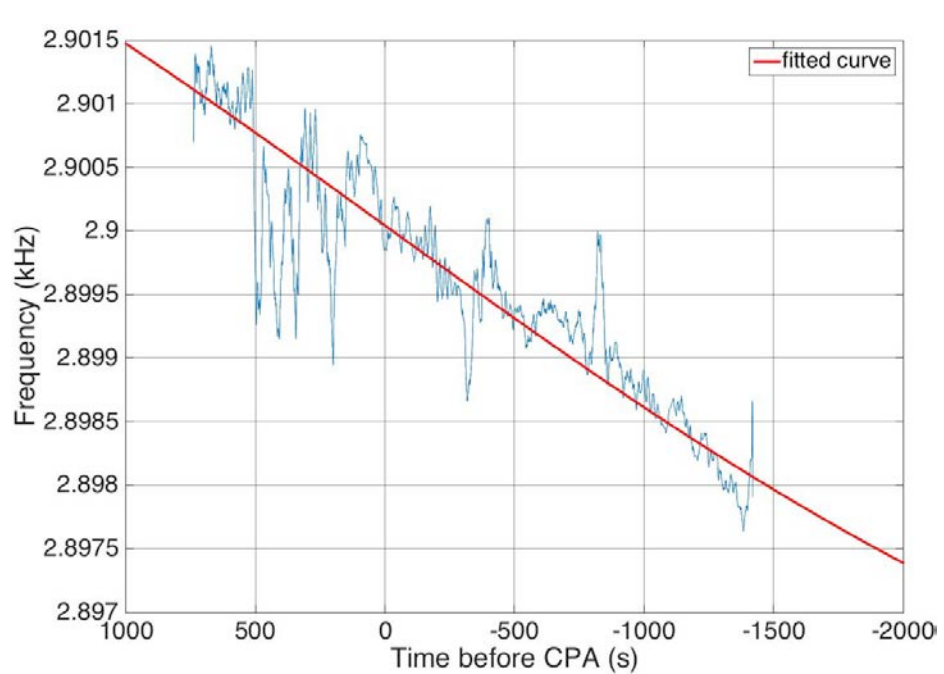


Figure 16. Time-Frequency Plot with Fadeout

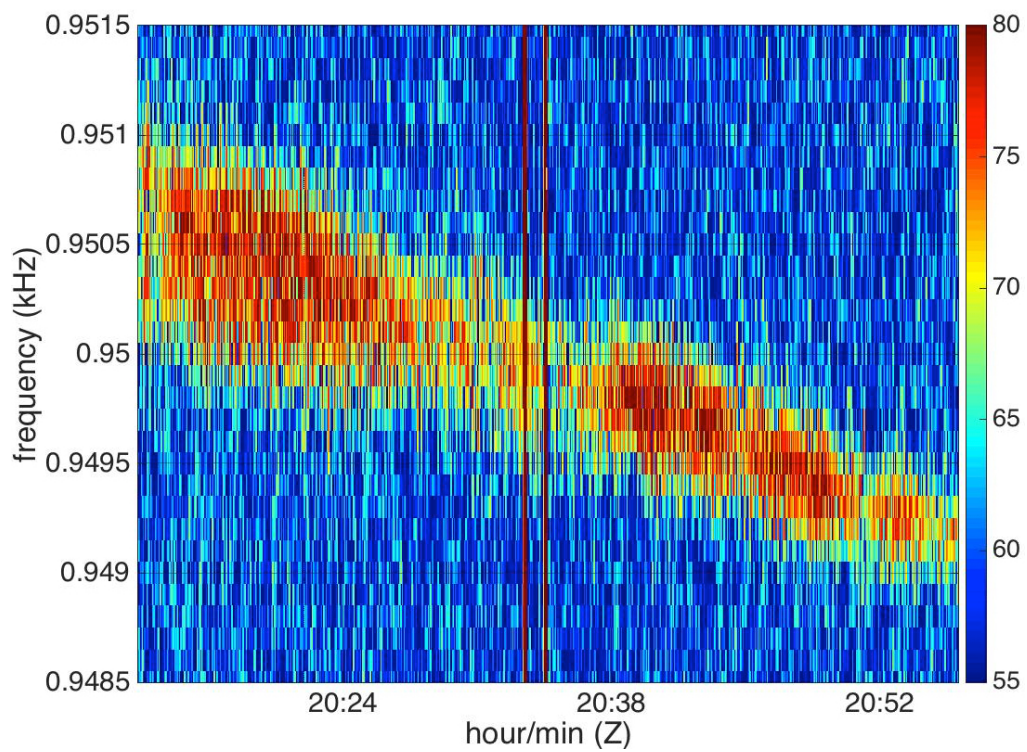


Figure 17. Spectrogram with More Signal Uncertainty

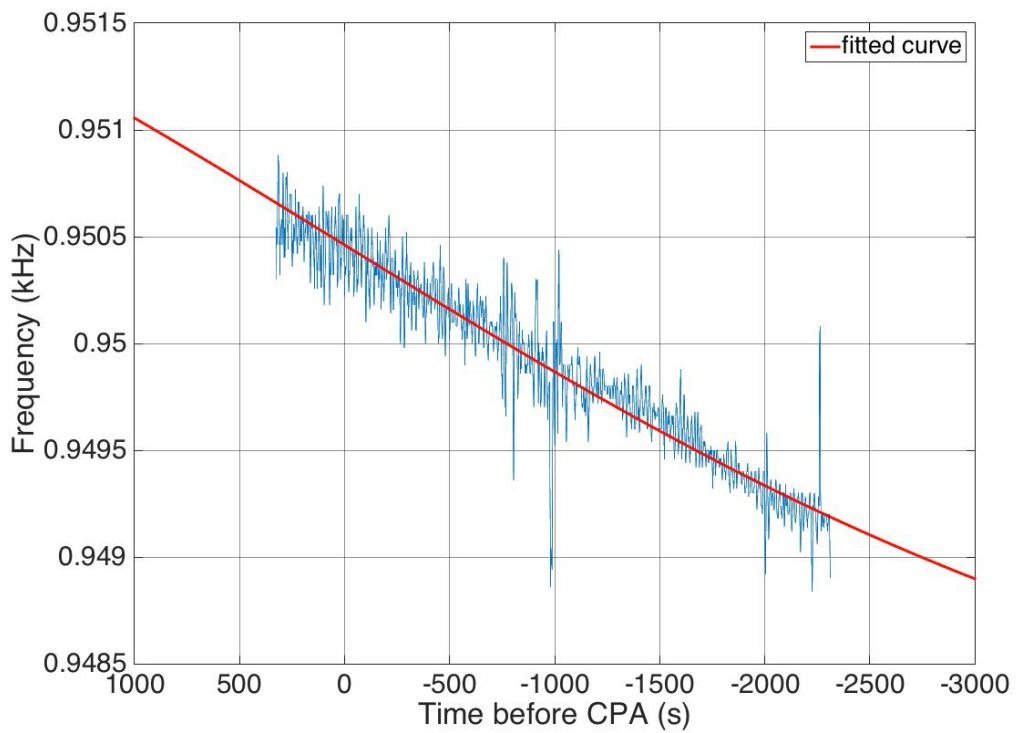
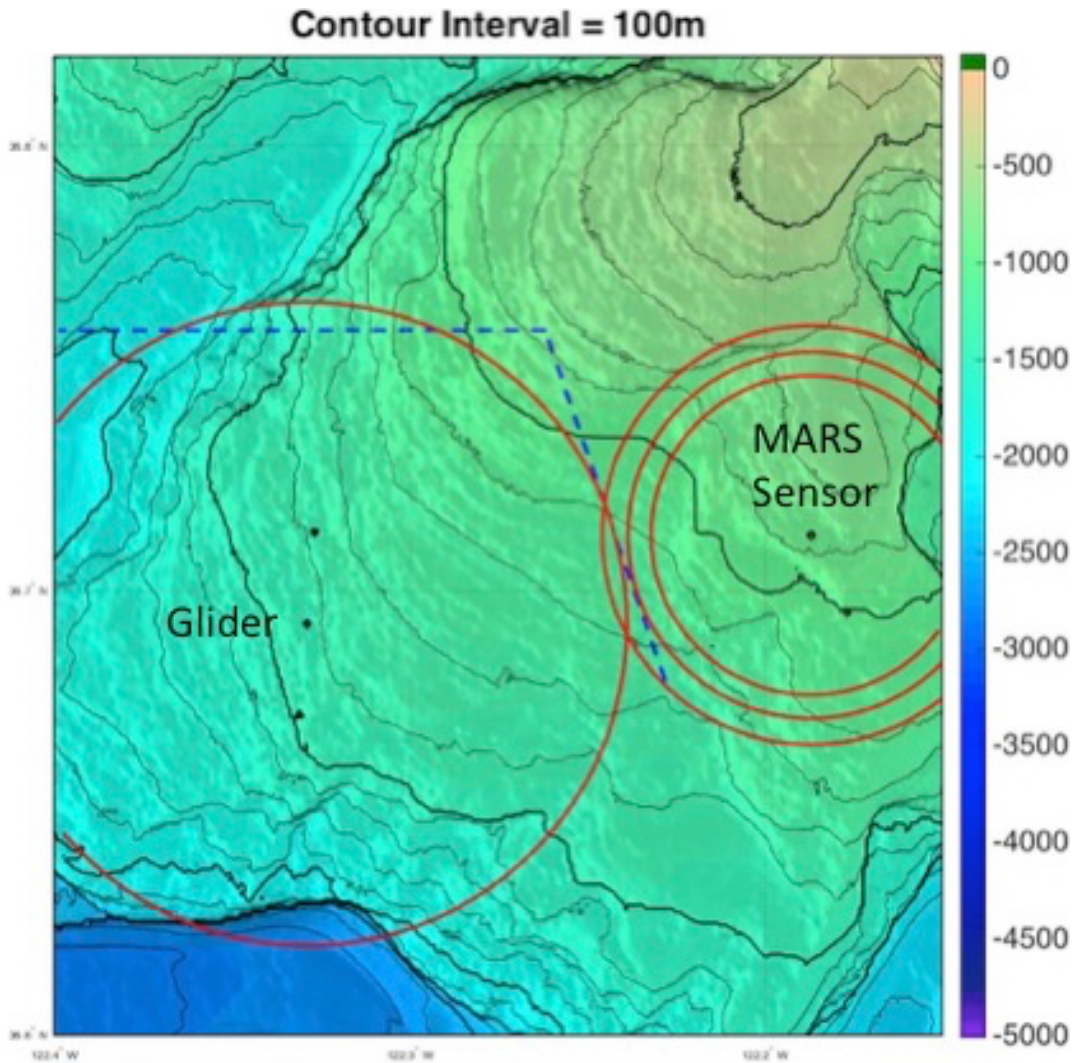


Figure 18. Frequency-Time Plot With Greater Signal Uncertainty

C. RECONSTRUCTION OF EMATT TRACK

By combining CPA distances from the more successful fits, a comparison can be made between predicted CPA and the ‘ground truth’ EMATT track. The estimated EMATT speed was also compared to programmed speed for the experiment.

Figure 19 displays sensor locations, estimated CPA distances, and programmed EMATT track from its launch point. The results of Doppler frequency shift parameter estimates are plotted as distance rings around their respective sensors. These rings are consistent with the programmed track of the EMATT.



The range circle around the estimated glider location (left diamond) corresponds to a radial distance of 8.1 km. The three range circles around the MARS sensor (right diamond) correspond to radial distances of 4.0 km, 4.5 km and 5.2 km. The blue dashed line corresponds to the EMATT programmed track.

Figure 19. Programmed EMATT Track and Sensor Layout with CPA Range Circles

D. SPEED DETERMINATION

The EMATT speed was set to be constant for this study at 5 kts (2.572 m/s) between maneuvers. Comparison of function fit parameters to this value yields another measure of the quality of the function fits. Typical estimated speed values for successful fits ranged from 2.3 m/s to 2.9 m/s.

VI. CONCLUSIONS

The use of networked USV/UUV acoustic receivers shows promise for detecting submerged sound sources and determining their track through analysis of detected Doppler shift. The source was detected by a glider-mounted hydrophone at a distance of 8 km and the MARS receiver at a distance of 4.5 km. These detection distances demonstrate the advantage of glider-mounted receivers at depths such as 900 m in downwardly refracting environments similar to Monterey Bay. Speed values for successful parameter estimates were within 15% of the programmed source speed. The parameter estimates for the successful data analysis were consistent with the programmed source behavior and source launch point.

For the runs that were less successful at yielding reasonable values for estimated parameters, the primary issues identified were: low SNR during parts of a run, erratic source behavior, or self-noise. This technique of parameter estimation via sequential localization could be improved by boosting SNR through more advanced methods of signal processing (to include handling fadeouts) or use of a more sophisticated acoustic sensor. Erratic source behavior could be improved by using different mobile acoustic sources. Of note, by requiring solutions of the form of Equation 3 and Figure 1, one can detect when the assumption of a linearly travelling source is no longer valid.

Arranging underwater sensors around a moving source track allows for reconstruction of that source track with sequential localization. Additionally, a sensor arrangement such as this would not require the precise time synchronization of conventional hydrophone arrays, enabling a wide distribution of networked system components with a larger detection coverage area.

One challenge to implementation of integrated UUV sensors demonstrated here is self-noise of the UUV system. Running a UUV glider in drift

mode for collection reduces the frequency of internal components activating and producing self-noise, suggesting this as the desired mode for collection.

The long loitering times (days) and acoustic path associated with persistent operation at depth where higher SNR values can be obtained makes the use of networked UUVs advantageous for the purpose of underwater acoustic detection. The detection ranges in this study for relatively unsophisticated single omni-directional hydrophones suggest the viability of utilizing more sophisticated sensors mounted on long loitering UUVs in networks of reasonable numbers of drones. One can expect UUVs with more sophisticated payloads could cover large areas of ocean for acoustic source detection and localization.

LIST OF REFERENCES

Acoustimetrics, 2013: Acousonde 3A brochure with specifications. Accessed August 23, 2017, http://www.acousonde.com/downloads/Acousonde_3A_Brochure.pdf.

Baumgartner, M. F., K. M. Stafford, P. Winsor, H. Statscewich, and D. M. Fratantoni, 2014: Glider-based passive acoustic monitoring in the Arctic. *Mar. Technol. Soc. J.*, **48**, 5, 40–51.

Chan, Y. T., and J. J. Towers, 1992: Sequential localization of a radiating source by Doppler-shifted frequency measurements. *IEEE Trans. Aerosp. Electron. Syst.*, **28**, **4**, 1084–1090.

Joseph, J. E., and D. Horner, 2014: Integration and optimization of UUV/USV operations in environmental characterization. Unpublished N2/N6 NPS research proposal.

Maguer, A., R. Dymond, A. Grati, R. Stoner, P. Guerrini, L. Troiano, and A. Alvarez, 2013: Ocean gliders payloads for persistent maritime surveillance and monitoring. *Oceans*, San Diego, CA, IEEE Oceanic Eng. Soc., 8 pp. doi:10.23919/OCEANS.2013.6740952.

MBARI, 2017a: Monterey Accelerated Research System (MARS). Accessed 24 Aug 2017, <http://www.mbari.org/at-sea/cabled-observatory/>.

MBARI, 2017b: Hydrophone for passive acoustic monitoring. Accessed 24 Aug 2017, <http://www.mbari.org/technology/solving-challenges/persistent-presence/mars-hydrophone/>.

Nott, B., 2015: Long-endurance maritime surveillance with ocean glider networks. M.S. thesis, Department of Oceanography, Naval Postgraduate School, 71 pp.

Send, U., L. Regier, and B. Jones, 2013: Use of underwater gliders for acoustic data retrieval from subsurface oceanographic instrumentation and bidirectional communication in the deep ocean. *J. Atmos. Oceanic Technol.*, **30**, 984–998, doi:10.1175/JTECH-D-11-00169.1.

THIS PAGE INTENTIONALLY LEFT BLANK

INITIAL DISTRIBUTION LIST

1. Defense Technical Information Center
Ft. Belvoir, Virginia
2. Dudley Knox Library
Naval Postgraduate School
Monterey, California